symmetry

IMPACT FACTOR 2.940

CITESCORE 4.3

Article

*E*0 Transition Strengths in ^{70}Se and ^{70}Kr Mirror Nuclei within a Beyond-Mean-Field Model

Alexandrina Petrovici

Special Issue

Selected Papers from Shapes and Symmetries in Nuclei: From Experiment to Theory (SSNET'21 Conference)

Edited by

Prof. Dr. Costel Petrache and Prof. Dr. Jerzy Dudek

MDPI

https://doi.org/10.3390/sym14122594

symmetry

MDPI

Article

*E*0 Transition Strengths in ^{70}Se and ^{70}Kr Mirror Nuclei within a Beyond-Mean-Field Model

Alexandrina Petrovici

Horia Hulubei National Institute for Physics and Nuclear Engineering, R-077125 Bucharest, Romania; spetro@nipne.ro; Tel.: +40-21-4042392

Abstract: The shape coexistence and mixing and the strengths of the *E*0 transitions in the mirror nuclei ^{70}Se and ^{70}Kr are investigated in the frame of the beyond-mean-field *complex* Excited Vampir model with variation after symmetry projection. The effective interaction is obtained renormalizing a nuclear matter G-matrix derived from the charge dependent Bonn CD potential in a rather large model space. The effects of shape mixing on the *E*0 transition strengths for the lowest few 0^+, 2^+, and 4^+ states as well as the *M*1 and *E*2 strengths for the $2_i^+ \rightarrow 2_j^+$ and $4_i^+ \rightarrow 4_j^+$ transitions are presented and discussed.

Keywords: shape coexistence; beyond-mean-field approach; *E*0 transition strengths; proton-rich medium mass nuclei

Citation: Petrovici, A. *E*0 Transition Strengths in ^{70}Se and ^{70}Kr Mirror Nuclei within a Beyond-Mean-Field Model. *Symmetry* **2022**, *14*, 2594. https://doi.org/10.3390/sym14122594

Academic Editors: Maxim Y. Khlopov and Tomohiro Inagaki

Received: 3 November 2022
Accepted: 6 December 2022
Published: 8 December 2022

1. Introduction

Intense theoretical and experimental effort are presently devoted to the investigation of the distinctive features of proton-rich nuclei in the A = 70 mass region dominated by shape coexistence. Their characteristic properties are essentially affected by the development of shape mixing with increasing excitation energy and spin and significantly influenced by the competing neutron–proton pairing correlations in both T = 0 and T = 1 channels and the like-nucleon ones, as well as the isospin symmetry breaking interactions. The nuclei situated in the vicinity of the N = Z line in this mass region exhibit a particularly wide variety of coexistence phenomena. The electric monopole transitions (*E*0) are a sensitive probe for the realistic understanding of the shape coexistence and mixing effects. The description of the coexisting configurations displaying different intrinsic deformations in the structure of the involved wave functions is a challenge and test for nuclear models. In recent years, *E*0 transitions have become a key observable in experiments and theoretical investigations [1–11]. More frequently, the *E*0 transitions between the 0^+ states have been studied, but recently *E*0 transition strengths for the lowest few 2^+ and 4^+ states have been considered relevant fingerprints of shape coexistence and mixing. In the A = 70 region, shape coexistence and mixing have progressively become the fundamental defining characteristics of proton-rich nuclei [2–5,11–19].

Recently, we investigated, in the frame of the *complex* Excited Vampir beyond-mean-field variational model, the interplay between the shape coexistence and isospin–symmetry breaking effects on the characteristics of the A = 70 and A = 74 isovector triplets as well as the beta-decay properties of ^{70}Br to ^{70}Se [13–15]. This work represents an extension of our investigations within the *complex* Excited Vampir model concerning the effects of shape coexistence and mixing on the characteristic properties of the ^{70}Se and ^{70}Kr mirror nuclei considering the issue of *E*0 transitions. The next section presents the essential features and the variational procedure underlying the *complex* Excited Vampir model. Section 3 presents and discusses the influence of shape coexistence and mixing displayed by the structure of the wave functions on particular observables and the *E*0 transition strengths for the lowest few 0^+, 2^+, and 4^+ states in the ^{70}Se and ^{70}Kr mirror nuclei. Some conclusions are drawn in Section 4.

2. Theoretical Framework

The variational model *complex* Excited Vampir (EXVAM) uses as basic building blocks Hartree–Fock–Bogoliubov (HFB) vacua. The corresponding HFB transformations are essentially *complex* and allow for neutron–proton, angular momentum, and parity mixing being restricted by axial symmetry and time-reversal invariance. The essentially *complex* unitary transformations account for natural- as well as unnatural-parity two-body correlations along with neutron–proton pairing correlations in both T = 1 and T = 0 channels already at the mean-field level. The restoration of broken symmetries, nucleon numbers, total angular momentum, and parity is done before variation using projection techniques. Within the Excited Vampir variational procedure, the symmetry-projected many-nucleon configurations are used as test wave functions in independent chains of variational calculations built for each symmetry. Within this procedure, one obtains the underlying HFB transformations as well as the mixing of the configurations ([13] and references therein). The *complex* Excited Vampir model allows for the use of realistic effective interactions in large model spaces exceeding the abilities of the shell-model configuration-mixing approach, creating the possibility to accomplish *large-scale* nuclear structure investigations.

In the present study, I used the same effective interaction and model space involved in our studies concerning shape coexistence effects on the structure and dynamics of exotic nuclei in the A = 70 region ([13–15] and references therein). The model space above the ^{40}Ca core is built out of the $1p_{1/2}$, $1p_{3/2}$, $0f_{5/2}$, $0f_{7/2}$, $1d_{5/2}$, and $0g_{9/2}$ oscillator orbitals for both neutrons and protons. One begins with an isospin symmetric basis and then one adds to the proton single-particle levels the Coulomb shifts induced by the ^{40}Ca core obtained by spherically symmetric Hartree–Fock calculations involving the D1S Gogny-interaction and a 21 major-shell basis [13]. The effective two-body interaction is obtained by the renormalization of a nuclear matter G-matrix derived from the charge-dependent Bonn CD potential. Short-range (0.707 fm) Gaussians are added in the T = 0 and T = 1 channels to enhance the pairing correlations. To influence the prolate–oblate competition and the onset of deformation, monopole shifts of -500 keV have been added to the matrix elements, having the form $\langle 1p1d_{5/2}; IT = 0|\hat{G}|1p1d_{5/2}; IT = 0\rangle$, where 1p indicates either the $1p_{1/2}$ or the $1p_{3/2}$ orbit, and of -370 keV to $\langle 0g_{9/2}0f; IT = 0|\hat{G}|0g_{9/2}0f; IT = 0\rangle$, where 0f indicates either the $0f_{5/2}$ or the $0f_{7/2}$ orbital [13]. Included in the Hamiltonian are the two-body matrix elements of the Coulomb interaction between the valence protons.

3. Results and Discussion

3.1. ^{70}*Se*

For the study of the structure and dynamics of the lowest few 0^+, 2^+, and 4^+ states in ^{70}Se, up to 22 orthogonal *complex* Excited Vampir configurations have been independently built for each considered symmetry. For each spin, the final solutions displaying the mixing of configurations of different deformations in the intrinsic system have been obtained by the diagonalization of the residual interaction between the corresponding many-nucleon EXVAM wave functions. The EXVAM spectrum of the lowest few 0^+, 2^+, and 4^+ states is compared with the available data in Figure 1. For the explored lowest two 0^+, 2^+, and 4^+ states, the EXVAM spectrum indicates good agreement with the experimental one [20]. The development of the shape mixing with increasing excitation energy and spin is displayed by the structure of the wave functions for the analyzed states in Table 1. In this table, the contribution of differently deformed prolate (p) and oblate (o) EXVAM configurations in the intrinsic system as a percentage of the total amplitude is illustrated. The amount of mixing of the configurations contributing at least 2% to the structure of the wave function for a state of a given spin and parity are indicated in parentheses in decreasing order. The structure of the wave functions of the lowest six 0^+ states reveals a variable mixing of configurations characterized by prolate and oblate deformation in the intrinsic system. Almost equal prolate and oblate content characterizes the ground state (altogether 53% oblate content, including the configurations that each contribute less than 2%) and the first excited state (altogether 55% prolate content, including the configurations that each

contribute less than 2%); the third, the fourth, and the sixth state are dominated by prolate deformed configurations, whereas the fifth 0^+ state is dominated by oblate ones.

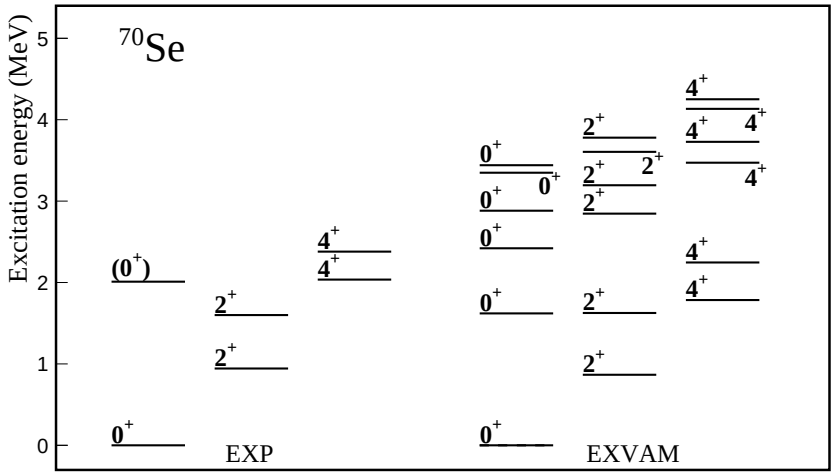

Figure 1. *Complex* Excited Vampir spectrum of the lowest few 0^+, 2^+, and 4^+ states in ^{70}Se (EXVAM) compared with the data [20] (EXP).

The configuration mixing for the investigated 2^+ states indicates prolate dominating content for the yrast (altogether 58% prolate configurations) and the sixth state, oblate dominating one for the second 2^+ state, almost equal prolate and oblate contribution for the fourth state, almost pure prolate mixing for the third 2^+, and almost pure oblate one for the fifth state. Similar behavior characterizes the lowest five 4^+ states, but oblate dominant content is obtained for the sixth state. For the spin 2^+, the quadrupole deformation parameter is changing from $\beta_2 = -0.28$ to $\beta_2 = -0.31$ for the oblate deformed EXVAM configurations, whereas for the prolate ones, it is changing from $\beta_2 = 0.32$ to $\beta_2 = 0.35$.

Table 1. The amount of mixing for the lowest *complex* Excited Vampir 0^+, 2^+, 4^+ states in ^{70}Se.

I[$\hbar$]	p	o	I[$\hbar$]	p	o	I[$\hbar$]	p	o
0_1^+	41(4)	51	2_1^+	56(2)	39(2)	4_1^+	52(2)	43(2)
0_2^+	51(3)	38(3)(2(2)	2_2^+	39	58	4_2^+	44	55
0_3^+	78(3)	6(6)(3)	2_3^+	94		4_3^+	87(5)(2)	
0_4^+	56(7)(2)	24(6)(2)	2_4^+	47	45	4_4^+	47 (6)	40
0_5^+	17(5)(2)(2)	47(17)(6)	2_5^+	4(2)	84(9)	4_5^+	10(2)	79(4)(4)
0_6^+	57	28(9)(3)	2_6^+	45(16)	24(6)(5)	4_6^+	27(9)	45(15)

The variety of mixing of the differently deformed prolate and oblate configurations in the structure of the 2^+ and 4^+ states is reflected by the spectroscopic quadrupole moments presented in Table 2. Based on the experimental data in the mass region, effective charges of $e_p = 1.2$ and $e_n = 0.2$ were used. The third and the fifth 2^+ and 4^+ states dominated ($\sim$90% contribution) by configurations of prolate and oblate deformation in the intrinsic system, respectively, manifest large spectroscopic quadrupole moments. The other investigated low-lying 2^+ and 4^+ states showing strong prolate–oblate mixing of differently deformed configurations are characterized by small positive or negative spectroscopic quadrupole moments. The first experimental investigations on the spectroscopic quadrupole moment of the yrast 2^+ state in ^{70}Se concluded that there is no evidence for oblate shape [16]. Improved experimental results indicate evidence for oblate shapes and suggest shape coexistence scenario for low spin states in ^{70}Se [17].

Table 2. Spectroscopic quadrupole moments (efm^2) for the lowest *complex* Excited Vampir 2^+ and 4^+ states in ^{70}Se.

I[$\hbar$]	Q_{sp}	I[$\hbar$]	Q_{sp}
2_1^+	−5.9	4_1^+	−6.4
2_2^+	2.6	4_2^+	−0.1
2_3^+	−41.6	4_3^+	−56.6
2_4^+	−7.1	4_4^+	−9.4
2_5^+	38.0	4_5^+	41.4
2_6^+	−13.9	4_6^+	8.4

The EXVAM results show that, in ^{70}Se, shape coexistence and mixing are the dominant characteristics, not only for the investigated 0^+ states, but also for the lowest few 2^+ and 4^+ states. Consequently, we investigated the $E0$ transition strengths connecting not only the 0^+ states, but also the low-lying 2^+ and 4^+ states. Table 3 presents the strengths (ρ^2) for the calculated $E0$ transitions linking the EXVAM states larger than 5 milliunits. The strongest $E0$ transitions between the lowest 0^+ states connects the fourth and the second 0^+ state. Weaker transitions are linking the second 0^+ and the ground state as well as the higher lying and the lowest three 0^+ states. Concerning the $E0$ transitions between the 2^+ states, we found maximum strengths linking the second and the yrast 2^+ and the fourth to the second 2^+ state. Weaker transitions connect the higher lying 2^+ states with the lowest three 2^+ states. For the $E0$ transitions connecting the 4^+ states, maximum strength links the second and the yrast 4^+ state.

Table 3. The ρ^2 values for the lowest *complex* Excited Vampir 0^+, 2^+, and 4^+ states in ^{70}Se.

Transition		Transition		Transition	
$\rho^2(E0;0_2^+ \to 0_1^+)$	0.010	$\rho^2(E0;2_2^+ \to 2_1^+)$	0.010	$\rho^2(E0;4_2^+ \to 4_1^+)$	0.014
$\rho^2(E0;0_4^+ \to 0_1^+)$	0.007	$\rho^2(E0;2_3^+ \to 2_1^+)$	0.006	$\rho^2(E0;4_3^+ \to 4_1^+)$	0.006
$\rho^2(E0;0_4^+ \to 0_2^+)$	0.018	$\rho^2(E0;2_4^+ \to 2_1^+)$	0.005	$\rho^2(E0;4_3^+ \to 4_2^+)$	0.008
$\rho^2(E0;0_5^+ \to 0_3^+)$	0.009	$\rho^2(E0;2_3^+ \to 2_2^+)$	0.005	$\rho^2(E0;4_4^+ \to 4_2^+)$	0.006
$\rho^2(E0;0_6^+ \to 0_3^+)$	0.010	$\rho^2(E0;2_4^+ \to 2_2^+)$	0.011		
		$\rho^2(E0;2_6^+ \to 2_3^+)$	0.007		

The latest measurements concerning the $E2$ decay of the yrast states indicate for the $B(E2;\Delta I = 2)$ strengths the values 342(19) and 370(24) e^2fm^4 for the 2^+ and 4^+ states, respectively [17,19]. The corresponding calculated EXVAM values are 473 and 706 e^2fm^4 for the 2^+ and 4^+ states, respectively. The strong shape mixing identified in the structure of the wave functions for the 2^+ and 4^+ states could induce significant $B(E2;\Delta I = 0)$ transition strengths linking the EXVAM states displayed in Table 3. The strongest EXVAM $B(E2)$ values are connecting the lowest two states of spin 2^+ and 4^+, 636 and 617 e^2fm^4, respectively, and the experimental value for the first amounts to 565 (240) e^2fm^4 [20]. The significant $E2$ and $M1$, $\Delta I = 0$ EXVAM transition strengths decaying higher lying 2^+ states amount to: $B(E2;2_3^+ \to 2_2^+)$= 23 e^2fm^4; $B(E2;2_4^+ \to 2_2^+)$ = 64 e^2fm^4; $B(E2;2_6^+ \to 2_3^+)$ = 20 e^2fm^4 and for $M1$, $B(M1;2_4^+ \to 2_2^+)$ = 0.011 μ_N^2. The results for the 4^+ states indicate $B(E2;4_3^+ \to 4_2^+)$ = 30 e^2fm^4, $B(E2;4_4^+ \to 4_2^+)$ = 29 e^2fm^4, and for the M1 branches $B(M1;4_4^+ \to 4_2^+)$ = 0.042 μ_N^2. Experimental investigations concerning the $E0$ transitions in ^{70}Se are currently being performed at TRIUMF-ISAC.

3.2. ^{70}Kr

Our previous investigations on the interplay between shape coexistence and isospin-symmetry breaking effects in the A = 70 isovector triplet revealed a shape change along the isobars [13]. The evolution of the shape mixing in the structure of the analog states explains the anomaly identified in the Coulomb energy differences. Our studies concerning the effects of shape coexistence and mixing on the analog states are extended to investigate

the $E0$ transitions between the lowest few 0^+, 2^+, and 4^+ states in ^{70}Kr, the mirror nucleus of ^{70}Se. In independent variational chains, up to 22 *complex* Excited Vampir configurations for each spin have been built. The EXVAM spectrum presented in Figure 2 compares well with the available experimental results [18].

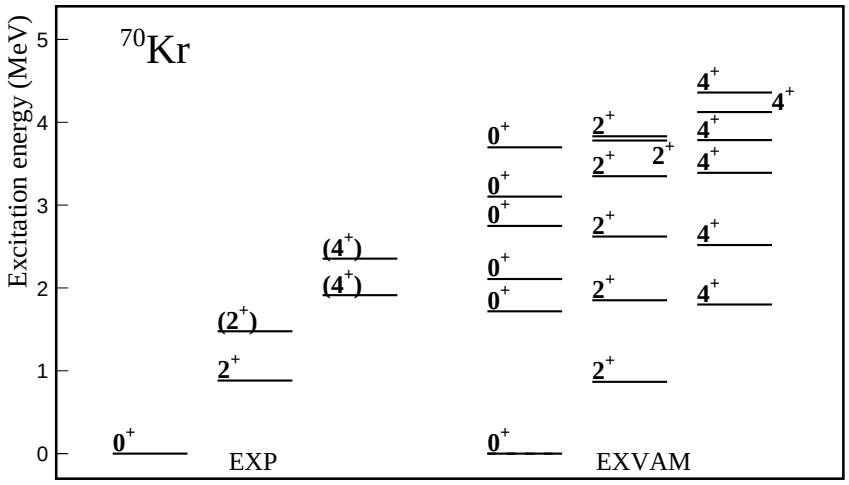

Figure 2. *Complex* Excited Vampir spectrum of the lowest 0^+, 2^+, and 4^+ states in ^{70}Kr (EXVAM) compared with the available data [18] (EXP).

The amount of mixing of differently deformed prolate and oblate EXVAM configurations in the structure of the lowest six 0^+, 2^+, and 4^+ states is presented in Table 4. The investigated states manifest, as in ^{70}Se, variable, in some cases very strong, prolate–oblate mixing, but the prolate content is larger for the corresponding states in ^{70}Kr. This feature appears already in the structure of the the wave functions of the analog states: the prolate content for the ground state, yrast 2^+, and yrast 4^+ state amounts to 72%, 73%, and 78%, respectively. For the spin 2^+, the quadrupole deformation parameter for the oblate EXVAM configurations varies from $\beta_2 = -0.27$ to $\beta_2 = -0.30$; for the prolate ones, from $\beta_2 = 0.30$ to $\beta_2 = 0.34$.

Table 4. The amount of mixing for the lowest *complex* Excited Vampir 0^+, 2^+, 4^+ states in ^{70}Kr.

I[$\hbar$]	p	o	I[$\hbar$]	p	o	I[$\hbar$]	p	o
0_1^+	69(3)	24(3)	2_1^+	70(3)	24	4_1^+	75(3)	19(2)
0_2^+	23(15)(4)(3)	47(2)	2_2^+	25	72	4_2^+	20	77
0_3^+	59(7)(2)	23(3)(2)	2_3^+	92(2)	2	4_3^+	91(3)(2)(2)	
0_4^+	51(16)(7)(4)	12(4)	2_4^+	31(2)	59(3)	4_4^+	36(4)	54(2)
0_5^+	41(6)(4)	41(3)	2_5^+	51(15)(3)	14(11)	4_5^+	44(10)(2)	39
0_6^+	54(11)(9)(2)	19	2_6^+	20(14)(11)(2)	28(19)(2)	4_6^+	54(14)(11)(9)(4)(3)	

The oblate–prolate mixing is reflected by the spectroscopic quadrupole moments of the investigated 2^+ and 4^+ states displayed in Table 5.

The strengths of the $E0$ transitions linking the investigated states larger than 5 milliunits are presented in Table 6. The trend in ^{70}Kr is similar to the one obtained for ^{70}Se, but the transition linking the lowest two 0^+ states is two times stronger. The EXVAM value for the $B(E2; 2_1^+ \rightarrow 0_1^+)$ amounts to 589 e^2fm^4, in good agreement with the measured value of 545 (90) e^2fm^4 [17,19]. Concerning the $B(E2; \Delta I = 0)$ transitions, the strongest connect the lowest two 2^+ and 4^+ states: 636 e^2fm^4 and 495 e^2fm^4, respectively. Significant $E2$ and $M1$, $\Delta I = 0$ EXVAM strengths for the higher lying 2^+ and 4^+ states are: $B(E2; 2_4^+ \rightarrow 2_2^+)$ = 41 e^2fm^4; $B(E2; 2_5^+ \rightarrow 2_4^+)$ = 422 e^2fm^4, $B(M1; 2_5^+ \rightarrow 2_4^+)$ = 0.018 μ_N^2, and $B(E2; 4_4^+ \rightarrow 4_2^+)$ = 31 e^2fm^4.

Table 5. Spectroscopic quadrupole moments (efm^2) for the lowest *complex* Excited Vampir 2^+ and 4^+ states in ^{70}Kr.

I[$\hbar$]	Q_{sp}	I[$\hbar$]	Q_{sp}
2_1^+	−21.9	4_1^+	−36.4
2_2^+	15.8	4_2^+	28.6
2_3^+	−45.6	4_3^+	−63.3
2_4^+	9.5	4_4^+	3.6
2_5^+	−25.8	4_5^+	−15.1
2_6^+	−2.8	4_6^+	−62.0

Table 6. The ρ^2 values for the lowest *complex* Excited Vampir 0^+, 2^+, and 4^+ states in ^{70}Kr.

Transition		Transition		Transition	
$\rho^2(E0;0_2^+ \to 0_1^+)$	0.021	$\rho^2(E0;2_2^+ \to 2_1^+)$	0.011	$\rho^2(E0;4_2^+ \to 4_1^+)$	0.011
$\rho^2(E0;0_4^+ \to 0_2^+)$	0.017	$\rho^2(E0;2_3^+ \to 2_1^+)$	0.005	$\rho^2(E0;4_4^+ \to 4_2^+)$	0.012
$\rho^2(E0;0_4^+ \to 0_3^+)$	0.009	$\rho^2(E0;2_4^+ \to 2_1^+)$	0.005	$\rho^2(E0;4_5^+ \to 4_2^+)$	0.005
$\rho^2(E0;0_5^+ \to 0_3^+)$	0.009	$\rho^2(E0;2_4^+ \to 2_2^+)$	0.015		
$\rho^2(E0;0_5^+ \to 0_4^+)$	0.010	$\rho^2(E0;2_5^+ \to 2_4^+)$	0.005		
$\rho^2(E0;0_6^+ \to 0_4^+)$	0.011	$\rho^2(E0;2_6^+ \to 2_5^+)$	0.006		
$\rho^2(E0;0_6^+ \to 0_5^+)$	0.006				

4. Conclusions

This paper presents the first results on the effect of shape coexistence and mixing on the $E0$ transitions linking the lowest few 0^+, 2^+, and 4^+ states in the ^{70}Se and ^{70}Kr mirror nuclei in the frame of the beyond-mean-field *complex* Excited Vampir model using an effective interaction based on the charge dependent Bonn CD potential. These investigations extend our successful studies on the characteristic features of the A = 70 isovector triplet accomplished within the same theoretical framework. The results reveal some significant $E0$ transitions as well as $E2$ and $M1$, $\Delta I = 0$ branches for the decay of the lowest 2^+ and 4^+ states. Strong similarities have been found in the behavior of the investigated observables for the two mirror nuclei. The increased contribution of the prolate deformed configurations in the structure of the wave functions going from ^{70}Se to ^{70}Kr is specifically revealed by the investigated observables. Experimental studies on the $E0$ transitions in ^{70}Se developed at TRIUMF-ISAC, Canada could confirm the shape coexistence and mixing scenario presented in the present work.

Funding: This research received no external funding.

Data Availability Statement: Not applicable.

Acknowledgments: This work was supported by a grant of the Ministry of Research, Innovation and Digitization, CNCS-UEFISCDI, project number PN-III-P4-PCE-2021-0060, within PNCDI III and Contract no. 9, EXONTEX-ISOLDE-CERN/2022.

Conflicts of Interest: The author declares no conflict of interest.

References

1. Wood, J.L.; Zganjar, E.F.; De Coster, C.; Heyde, K. Electric monopole transitions from low energy excitations in nuclei. *Nucl. Phys. A* **1999**, *651*, 323. [CrossRef]
2. Chandler, C.; Regan, P.H.; Pearson, C.J.; Blank, B.; Bruce, A.M.; Catford, W.N.; Curtis, N.; Czajkowski, S.; Gelletly, W.; Grzywacz, R.; et al. Evidence for a highly deformed oblate 0^+ state in $^{74}_{36}$Kr. *Phys. Rev. C* **1997**, *56*, R2924. [CrossRef]
3. Petrovici, A.; Schmid, K.W.; Faessler A. Microscopic aspects of shape coexistence in ^{72}Kr and ^{74}Kr. *Nucl. Phys. A* **2000**, *665*, 333. [CrossRef]
4. Becker, F.; Korten, W.; Butler, P.A.; Hannachi, F.; Paris, P.; Buforn, N.; Chandler, C.; Jansen, A.; Houry, M.; Hübel, H.; et al. Investigation of $E0$ transition in ^{74}Kr. *Phys. Scr.* **2000**, *T88*, 17. [CrossRef]
5. Bouchez, E.; Matea, I.; Korten, W.; Becker, F.; Blank, B.; Borcea, C.; Buta, A.; Emsallem, A.; De France, G.; Genevey, J.; et al. New shape isomer in the self-conjugate nucleus ^{72}Kr. *Phys. Rev. Lett.* **2003**, *90*, 082502. [CrossRef] [PubMed]

6. Peters, E.E.; Prados-Estévez, F.M.; Chakraborty, A.; Mynk, M.G.; Bandyopadhyay, D.; Choudry, S.N.; Crider, B.P.; Garrett, P.E.; Hicks, S.F.; Kumar, A.; et al. *E*0 transitions in ^{106}Pd: Implications for shape coexistence. *Eur. Phys. J. A* **2016**, *52*, 96. [CrossRef]
7. Evitts, L.J.; Garnsworthy, A.B.; Kibédi, T.; Smallcombe, J.; Reed, M.W.; Brown, B.A.; Stuchbery, A.E.; Lane, G.J.; Eriksen, T.K.; Akber, A.; et al. Identification of significant *E*0 strength in the $2_2^+ \rightarrow 2_1^+$ transitions of ^{58,60,62}Ni. *Phys. Lett. B* **2018**, *779*, 396. [CrossRef]
8. Smallcombe, J.; Berean-Dutcher, J.; Moukaddam, M.; Garnsworthy, A.B.; Andreoiu, C.; Caballero-Folch, R.; Drake, T.E.; Evitts, L.J.; Hackman, G.; Henderson, J.; et al. *E*0 transition strength in ^{110}Pd. *Eur. Phys. J. A* **2018**, *54*, 165. [CrossRef]
9. Evitts, L.J.; Garnsworthy, A.B.; Kibedi, T.; Smallcombe, J.; Reed, M.W.; Stuchbery, A.E.; Lane, G.J.; Eriksen, T.K.; Akber, A.; Alshahrani, B.; et al. *E*0 transition strength in stable Ni isotopes. *Phys. Rev. C* **2019**, *99*, 024306. [CrossRef]
10. Kibedi, T.; Garnsworthy, A.B.; Wood, J.L. Electric monopole transitions in nuclei. *Prog. Part. Nucl. Phys.* **2022**, *123*, 103930. [CrossRef]
11. Smallcombe, J.; Garnsworthy, A.B.; Korten, W.; Singh, P.; Ali, F.A.; Andreoiu, C.; Ansari, S.; Ball, G.C.; Barton, C.J.; Bhattacharjee, S.S.; et al. Improved measurement of the $0_2^+ \rightarrow 0_1^+$ *E*0 transition strength for ^{72}Se using SPICE spectrometer. *Phys. Rev. C* **2022**, *106*, 014312. [CrossRef]
12. Obertelli, A.; Baugher, T.; Bazin, D.; Delaroche, J.-P.; Flavigny, F.; Gade, A.; Girod, M.; Glasmacher, T.; Goergen, A.; Grinyer, G.F.; et al. Shape evolution in self-conjugate nuclei, and the transitional nucleus ^{68}Se. *Phys. Rev. C* **2009**, *80*, 031304(R). [CrossRef]
13. Petrovici, A. Isospin-symmetry breaking and shape coexistence in A$\sim$ 70 analogs. *Phys. Rev. C* **2015**, *91*, 014302. [CrossRef]
14. Petrovici, A.; Andrei O. Weak interaction rates and shape coexistence for the Z = N + 2 isotopes ^{70}Kr and ^{74}Sr. *Phys. Rev. C* **2015**, *92*, 064305. [CrossRef]
15. Petrovici, A. Shape coexistence and β decay of ^{70}Br within a beyond-mean-field approach. *Phys. Rev. C* **2018**, *97*, 024313. [CrossRef]
16. Hurst, A.M.; Butler, P.A.; Jenkins, D.G.; Delahaye, P.; Wenander, F.; Ames, F.; Barton, C.J.; Behrens, T.; Bürger, A.; Cederkäll, J.; et al. Measurement of the sign of the spectroscopic quadrupole moment for the 2_1^+ state in ^{70}Se: No evidence for oblate shape. *Phys. Rev. Lett.* **2007**, *98*, 072501. [CrossRef] [PubMed]
17. Ljungvall, J.; Görgen, A.; Girod, M.; Delaroche, J.-P.; Dewald, A.; Dossat, C.; Farnea, E.; Korten, W.; Melon, B.; Menegazzo, R.; Obertelli, A.; et al. Shape coexistence in light Se isotopes: Evidence for oblate shapes. *Phys. Rev. Lett.* **2008**, *100*, 102502. [CrossRef] [PubMed]
18. Wimmer, K.; Korten, W.; Arici, T.; Doornenbal, P.; Aguilera, P.; Algora, A.; Ando, T.; Baba, H.; Blank, B.; Boso, A.; et al. Shape coexistence and isospin symmetry in A=70 nuclei: Spectroscopy of the $T_z = -1$ nucleus ^{70}Kr. *Phys. Lett. B* **2018**, *785*, 441. [CrossRef]
19. Wimmer, K.; Korten, W.; Doornenbal, P.; Arici, T.; Aguilera, P.; Algora, A.; Ando, T.; Baba, H.; Blank, B.; Boso, A.; et al. Shape changes in the mirror nuclei ^{70}Kr and ^{70}Se. *Phys. Rev. Lett.* **2021**, *126*, 072501. [CrossRef] [PubMed]
20. Gurdal, G.; McCutchan, E.A. Nuclear data sheets for A = 70. *Nucl. Data Sheets* **2016**, *136*, 1. [CrossRef]